

PeV Cosmic Rays: A Window on the Leptonic Era?

Richard Wigmans¹

Department of Physics, Texas Tech University, Lubbock, TX 79409-1051, USA

Abstract

It is shown that a variety of characteristic features of the high-energy hadronic cosmic ray spectra, in particular the abrupt changes in the spectral index that occur around 3 PeV and 300 PeV, as well as the corresponding changes in elemental composition that are evident from kinks in the $\langle X_{\max} \rangle$ distribution, can be explained in great detail from interactions with relic Big Bang antineutrinos, provided that the latter have a rest mass of $\sim 0.5 \text{ eV}/c^2$.

Key words: Cosmic rays, Knee, Relic neutrinos, Neutrino mass

1 Introduction

The energy region between 1 and 10 PeV is an area of intense study in cosmic ray research. The all-particle cosmic-ray energy spectrum falls extremely steeply with energy. In general, it is well described by a power law

$$\frac{dN}{dE} \sim E^{-n} \quad (1)$$

with $n \approx 2.7$ for energies below 1 PeV. The steepening that occurs between 1 PeV and 10 PeV, where the spectral index n changes abruptly from 2.7 to 3.0, is known as the *knee* of the cosmic ray spectrum.

This phenomenon is generally believed to contain key information about the origin of the cosmic rays and about the acceleration mechanisms that play a role. Especially models in which the cosmic rays are resulting from particle acceleration in the shock waves produced in Supernova explosions have received much attention in the literature. Such models predict a maximum energy, proportional to the nuclear charge Z of the particles [1]. In the context of these models, the knee is assumed

¹ Email wigmans@ttu.edu, fax (806) 742-1182.

to be associated with this (Z -dependent) maximum and the corresponding cutoff phenomena. In the past years, major efforts have been mounted to determine the elemental composition of the cosmic rays in the knee region. These efforts have revealed that the knee coincides with an abrupt change in the elemental composition of the cosmic rays.

We would like to point out that the high-energy cosmic ray spectra contain several other remarkable features. For example, there is a significant second knee in the energy spectrum at ~ 300 PeV, which coincides with an abrupt change in the elemental composition as well. Even though these features are experimentally well established, they have received little or no attention in the literature, presumably because they do not fit in the context of the aforementioned shock wave acceleration models.

In this paper, we show that *all* measured features of the cosmic ray spectra in the energy range from 10^{14} eV to 10^{18} eV are in detailed agreement with the predictions of a completely different model. In this model, interactions between the cosmic rays and $\bar{\nu}_e$ remnants from the Big Bang play a crucial role. If this is correct, then the experimental cosmic ray data make it directly possible to determine the rest mass of these neutrinos. The result, $m_{\nu_e} = 0.5 \pm 0.2$ eV/ c^2 , falls inside the narrowing window still allowed by explicit measurements of this important parameter. If the role of interactions with relic neutrinos is indeed as important as suggested by the cosmic ray data, then this also provides crucial information about the possible origin of the PeV cosmic rays and about the acceleration mechanisms.

This paper is organized as follows. In Section 2, we review the key elements of the experimental cosmic ray information in the energy range from 10^{14} eV to 10^{18} eV. In Section 3, we describe how interactions with relic neutrinos might explain these phenomena. In Section 4, a possible scenario for the origin of PeV cosmic rays is discussed. Conclusions are given in Section 5.

2 Cosmic rays in the 0.1 – 1000 PeV range

All measurements in this energy range have been performed in extensive air-shower experiments. The detectors measure the Čerenkov light, the scintillation light and/or the charge produced by the shower particles generated in the absorption process that takes place in the Earth's atmosphere. Some experiments, *e.g.*, the Fly's Eye [2], are capable of reconstructing the shower profile in the atmosphere. This may provide important information about the type of particle that initiated the shower.

2.1 The knee

In the past 20 years, about a half-dozen experiments have measured the cosmic ray spectra in the energy range from 1 – 10 PeV. The existence of a kink in this area has been very well established. The different experiments agree on the fact that the observed change in the spectral index n is very significant and occurs very abruptly. As an example, Figure 1 shows the data from the CASA-BLANCA experiment [3], which recently performed measurements in the energy range from 0.3 PeV to 30 PeV at the Dugway site in Utah (U.S.A.), near the location of the Fly’s Eye detectors [4]. The spectral index was found to change from $n = 2.72 \pm 0.02$ at energies below 2 PeV to $n = 2.95 \pm 0.02$ above 2 PeV. Similarly significant kinks were reported by other experiments, *e.g.*, Akeno [5], Tibet AS γ [6] and DICE [7].

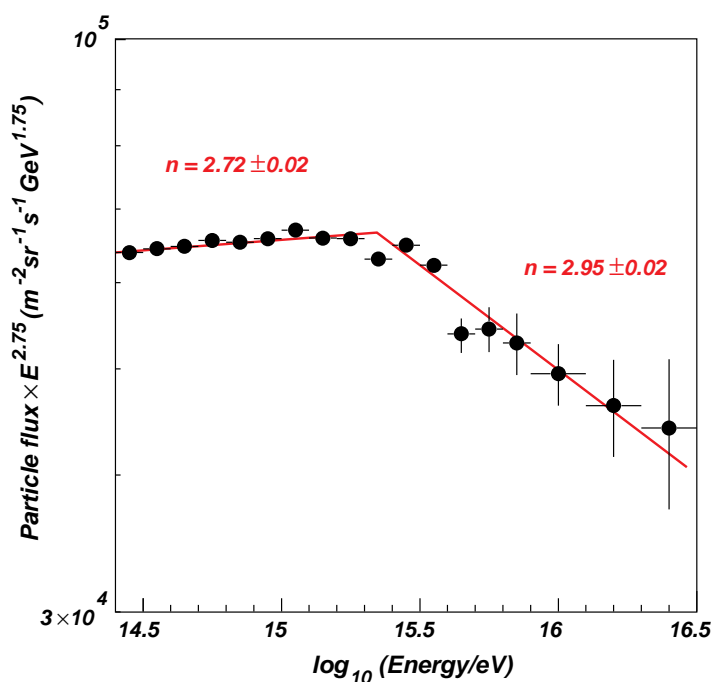


Fig. 1. The all-particle energy spectrum of cosmic rays, measured by the CASA-BLANCA experiment [3].

The abruptness of the change in the spectral index clearly suggests that some kind of threshold is crossed. However, the precise value of the threshold energy varies from one experiment to the next. This is undoubtedly a consequence of differences in the energy calibration methods of the experimental equipment that were applied in the different experiments. Given the absence of a reliable calibration source with precisely known energy in the PeV regime, it is no surprise that the absolute energy scales differ by as much as a factor of two. The reported values for the threshold energy range from 2 PeV (*e.g.*, for CASA-BLANCA) to 4 PeV (Akeno). In the following, we will adopt a value of 3 ± 1 PeV.

2.2 The kink near 300 PeV

Several extensive air-shower experiments that have studied the cosmic ray spectrum at the highest energies have reported a kink in the area around $\log E = 17.5$. The Fly's Eye experiment, which obtained the largest event statistics, observed a change in the spectral index from 3.01 ± 0.06 for energies $< 10^{17.5}$ eV to 3.27 ± 0.02 for energies $10^{17.5} < E < 10^{18.5}$ eV [8]. The Haverah Park experiment also reported a kink at $\log E = 17.6$, with the spectral index changing from 3.01 ± 0.02 to 3.24 ± 0.07 [9].

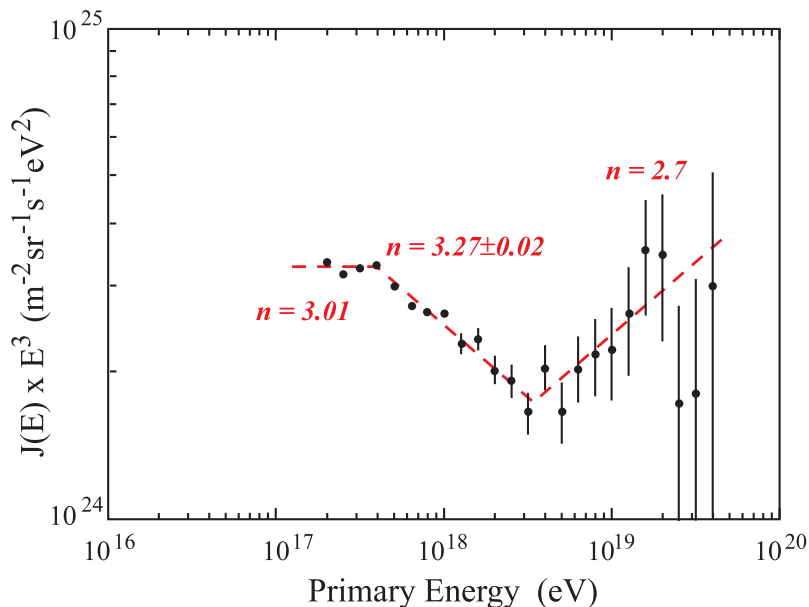


Fig. 2. The all-particle energy spectrum of cosmic rays, measured by the Fly's Eye experiment [8].

The Fly's Eye results are shown in Figure 2. In order to better discern the characteristic features, the differential energy spectrum has been multiplied by E^3 , as opposed to $E^{2.75}$ in Figure 1. Figure 2 shows several other interesting features, such as the *ankle* near $\log E = 18.5$, as well as several events above the GZK limit [10]. The authors of Reference [8] concentrated their attention entirely on these phenomena near the high-energy end of their experimental reach. However, the change of the spectral index near their low-energy limit is also very interesting.

The fact that the Fly's Eye detectors lacked sensitivity below 100 PeV limited the significance of their measurement of the change in the spectral index to about 4 standard deviations. However, the fact that several other experiments have measured n values of 2.95 - 3.00 with a precision of the order of 0.02 in the energy range from 5 - 100 PeV [3,9], while Fly's Eye measured $n = 3.27 \pm 0.02$ for energies between 300 and 3000 PeV makes the overall significance of this kink comparable with that of the knee around 3 PeV.

2.3 The elemental composition

Since the detectors in extensive air-shower experiments are located behind an absorber with a thickness of about 10 nuclear interaction lengths (the Earth's atmosphere), it is usually impossible to determine the identity of the incoming cosmic particle event by event. However, it is in some experiments possible to distinguish protons, α particles and heavier nuclei on a statistical basis. In experiments such as Fly's Eye [8], this is done by measuring the shower profile in the atmosphere. These profiles are, on average, quite different for the mentioned constituents of the cosmic ray spectra. In other experiments, *e.g.*, KASCADE [11], a large number of different shower characteristics are used simultaneously in a neural network that is trained to assign probabilities that the event was initiated by a proton, an α particle or a heavier nucleus on the basis of the experimental information.

One experimental parameter that is frequently used in this context is the average depth in the atmosphere at which the shower reaches its maximum intensity, $\langle X_{\max} \rangle$. At a given energy, $\langle X_{\max} \rangle$ is larger for protons than for heavier ions, and its value decreases as the nuclear charge Z of the projectiles increases. There are two reasons for these effects:

- (1) The *nuclear interaction length* (λ_{int}), *i.e.* the average distance the primary particle penetrates into the atmosphere before undergoing a nuclear interaction, is proportional to $A^{-2/3}$. Therefore, protons penetrate, on average, much deeper into the atmosphere than do heavier nuclei.
- (2) The *particle multiplicity* is smaller in reactions initiated by protons than in those initiated by heavier nuclei. Therefore, the energy of the incoming proton is transferred to a smaller number of secondaries, which carry thus, on average, more energy than the secondaries produced in reactions initiated by heavier ions of the same primary energy. And since the depth of the shower maximum increases with energy, the showers developed by the secondaries in proton-induced reactions reach their maximum intensity farther away from the primary vertex than in case of showers induced by heavier ions.

In summary, showers induced by protons of a given energy start later and peak at a larger distance from the primary vertex than showers induced by heavier ions of the same energy. These effects can be quantitatively estimated on the basis of the well known characteristics of showers at lower energy, for example in the following way [12].

The Particle Data Group lists the nuclear interaction length for protons in air as 90 g cm^{-2} [13]. Combined with the $A^{-2/3}$ cross section dependence, this leads to estimates of $\lambda_{\text{int}} = 36 \text{ g cm}^{-2}$ for α s and $\lambda_{\text{int}} = 6 \text{ g cm}^{-2}$ for iron nuclei in air. Therefore, effect 1 listed above will cause $\langle X_{\max} \rangle$ for proton-induced showers to be 54 g cm^{-2} larger than for α -induced showers and 84 g cm^{-2} larger than for showers induced by iron nuclei.

To estimate the second effect, it is important to realize that the maximum intensity in air showers is reached, in first approximation, at a depth where the electromagnetic showers developed by photons from decaying π^0 s produced in the *first* nuclear reaction reach their peak intensity. This is a consequence of the fact that the interaction length for charged pions in air is only ~ 4 times larger than the radiation length. In dense absorber materials, these two quantities may differ by as much as a factor of 30 and, as a result, hadron showers in dense detectors, such as calorimeters used in particle physics experiments, have very different characteristics [12]. The maximum intensity in a shower induced by a photon is approximately reached at a depth [14]:

$$t_{\max} = \ln y + 0.5 \quad (2)$$

where t_{\max} is expressed in radiation lengths (X_0) and y is the photon energy, expressed in units of the critical energy (ϵ_c). This relationship is graphically represented by the solid line in Figure 3 for photon-induced showers in air ($X_0 = 36.7 \text{ g cm}^{-2}$, $\epsilon_c = 87 \text{ MeV}$).

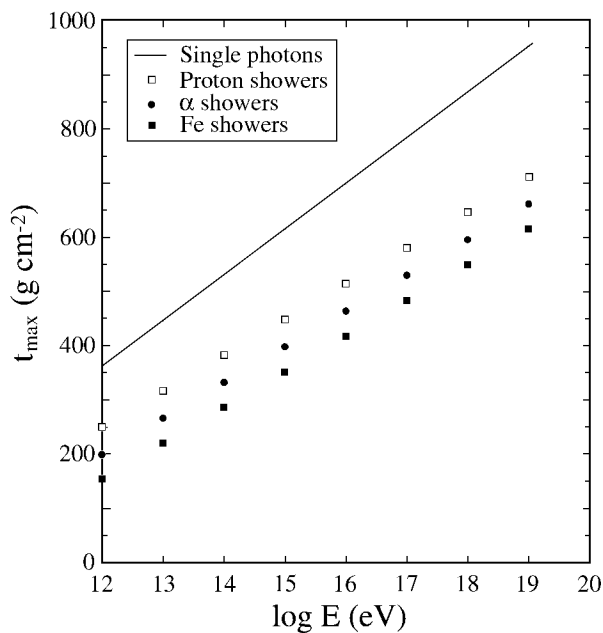


Fig. 3. The average depth of the shower maximum, calculated from the starting point of the showers, as a function of energy. Shown are the results for showers induced by single photons (Equation 2) and for the electromagnetic component of showers induced by protons, α s and Fe nuclei in the atmosphere. The latter were calculated on the basis of multiplicity assumptions discussed in the text.

In order to calculate the shower maximum in hadron-induced showers, we have to know the average fraction of the energy of the incoming particle that is transferred to individual photons. This may be derived from the multiplicity distributions measured in accelerator-based experiments.

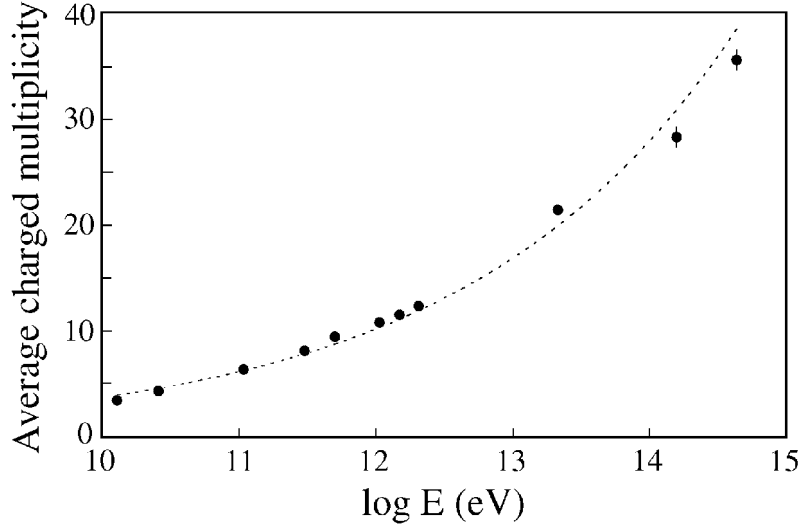


Fig. 4. The average charged particle multiplicity measured in pp reactions, as a function of energy. The dashed line represents the fit used to extrapolate these data to higher energies. See text for details.

Figure 4 shows the average multiplicity of charged particles produced in pp interactions as a function of energy [13,15]. Most of these data come from collider experiments and we have Lorentz-transformed these data to a fixed-target geometry. The dashed line is the result of an exponential fit and, for lack of a better method, we have used this fit to extrapolate to higher energies. The average photon energy in the proton-induced showers was calculated as follows. For example, at $\sqrt{s} = 546$ GeV, which corresponds to a fixed-target energy of $1.59 \cdot 10^{14}$ eV, the measured charged multiplicity was, on average, 28.3 ± 1.0 [15]. Assuming that equal numbers of π^+ s, π^- s and π^0 s are produced in the nuclear interactions, the total multiplicity is thus 42.5 and since a π^0 decays into 2 photons, these photons carry, on average, $1/85$ of the energy of the incoming proton. The average distance from the starting point of proton showers to the shower maximum was calculated at this energy on the basis of Equation 2, using a photon energy of $1.59 \cdot 10^{14}/85 = 1.87 \cdot 10^{12}$ eV. The other proton points (the open squares in Figure 3) were found in a similar way.

The points for showers induced by α particles and by iron nuclei were found by assuming that the other nucleons in the projectile would start simultaneous showers in the first nuclear interaction and that the initial energy would thus be shared among a correspondingly increased number of secondaries. This assumption is based on experimental observations in high-energy heavy-ion scattering experiments at CERN and Brookhaven. In the case of α -induced showers, we therefore increased the multiplicity by a factor of 4 and in the case of iron nuclei by a factor of 14, since the target nucleus (predominantly ^{14}N) only contains 14 nucleons. This simplifying approach overestimates the multiplicities. Therefore, the differences between showers induced by the different nuclei shown in Figure 3 represent an upper limit.

Figure 3 shows a logarithmic energy dependence of the shower maxima. This trend is somewhat modified when the effects of re-interacting charged pions are taken into account. Looking at Equation 2 and considering that $\lambda_{\text{int}}^{\pi} \approx 4X_0^2$, we see that such effects will tend to shift the shower maximum to a larger depth if the average charged particle multiplicity is less than ~ 50 (e^4). And since the average multiplicity increases with energy, this effect shifts the shower maximum more for lower-energy cosmic rays than for the highest-energy ones. In calculating the effects of re-interacting pions in the second, third, and higher generations of the shower development, we also have to take into account the fact that, as the pions become less energetic, they are also more likely to decay rather than to re-interact. For example, a 100 GeV π^+ produced at a depth of 150 g cm^{-2} has comparable probabilities to decay and to interact in the atmosphere. At higher altitude, the decay probability increases, at lower altitude the particle is more likely to interact.

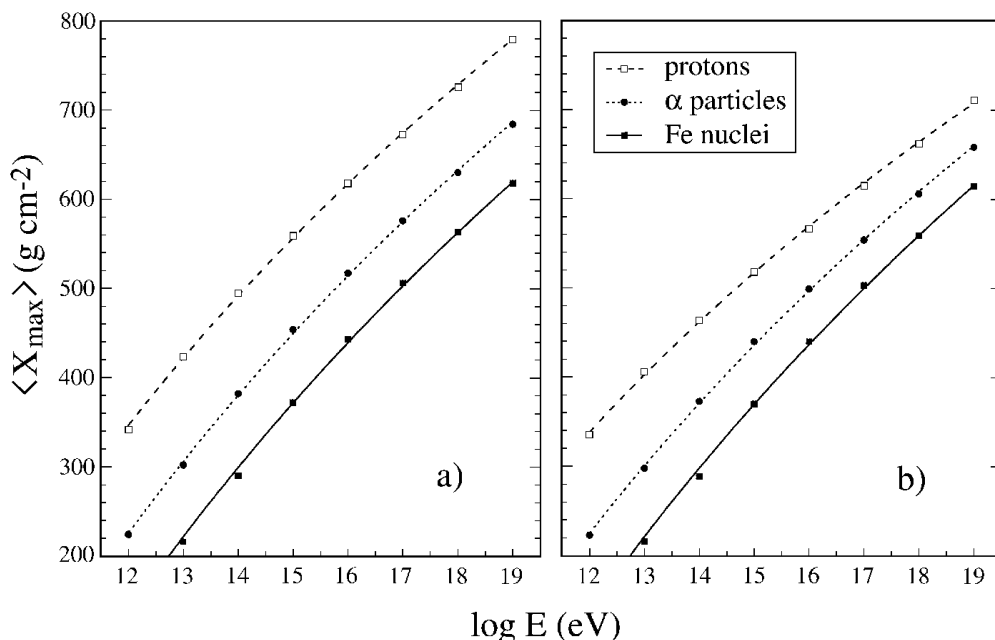


Fig. 5. The average depth inside the atmosphere at which the cosmic ray showers reach their maximum intensity. Results of calculations that were performed for a constant cross section (a) and for an energy dependent cross section (b). See text for details.

Figure 5a shows the results of a hand-based calculation, in which we have taken these effects into account for 4 generations of particle multiplication. The average depth of the shower maximum increases slower than logarithmically with energy. The curves for protons, α -particles and iron nuclei run more or less parallel to each other. The latter tendency changes when we also take into account the effect of a possible increase of the total cross section for the primary nuclear interactions with energy. According to the Particle Data Group [13,16], the total cross section for pp

² The interaction length for pions is larger than that for protons in the same material. Differences of 20% - 50% have been reported in the literature [12]

collisions gradually increases from 40 mb at 1 TeV to 120 mb at 10^{18} eV³. Therefore, the nuclear interaction length in air decreases by a factor of 3 over this energy range, from 90 g cm^{-2} at 1 TeV to 30 g cm^{-2} in the EeV range. The interaction lengths of the heavier nuclei are probably affected similarly. In Figure 5b, we have taken this effect into account as well. Obviously, it reduces the Z dependence of $\langle X_{\max} \rangle$ as the energy increases.

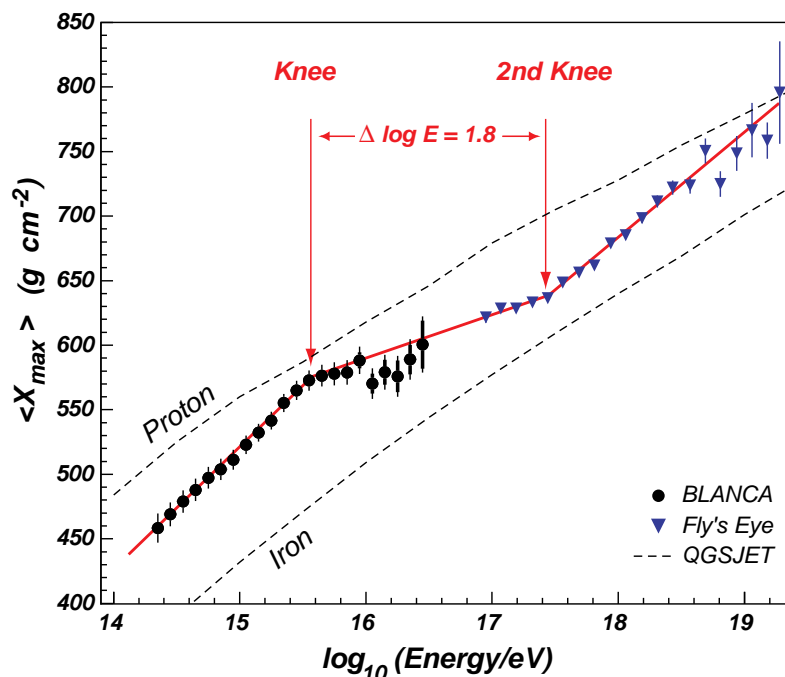


Fig. 6. The average depth of the shower maximum in the atmosphere as a function of the energy of the cosmic rays. Experimental data were obtained with the detectors of the BLANCA [3] and Fly's Eye [8] experiments. The dashed lines represent model calculations for protons and iron nuclei as the primary cosmic particles. See text for details.

The above discussion is intended as an introduction to the *experimental* $\langle X_{\max} \rangle$ data, which are shown in Figure 6, together with the results of model calculations performed by the authors of the papers in which these data were published [3,8].

Its purpose is to demonstrate three things:

- (1) The conclusions drawn from simple considerations based on a fundamental understanding of shower development are confirmed in detail by the results of very sophisticated and elaborate model calculations such as the QGSJET ones depicted in Figure 6.
- (2) The curve for α -induced showers is located in between those for protons and iron in Figure 6, somewhat closer to the iron curve than to the one for protons.
- (3) Since all effects contributing to these model curves lead to smooth changes as a function of energy, the two kinks observed in the experimental data (indi-

³ It should be noted that this trend hinges on the merits of a *single* experimental data point

cated by the arrows in Figure 6) represent a **very remarkable phenomenon**.

A kink in the $\langle X_{\max} \rangle$ distribution is strongly indicative for a threshold phenomenon, even more so than a kink in the primary energy spectra. The cosmic rays consist of a mixture of protons, α s and heavier nuclei. The threshold concerns a process that *selectively* affects one of these components. Therefore, the elemental composition abruptly starts to change when the threshold is passed. At low energies, protons are the most abundant particles. At the first kink, protons drop selectively out of the mix and heavier species start to dominate. At the second kink, this process is reversed: The protons start to come back and at the highest energies, they are again the most abundant components of the cosmic ray spectrum.

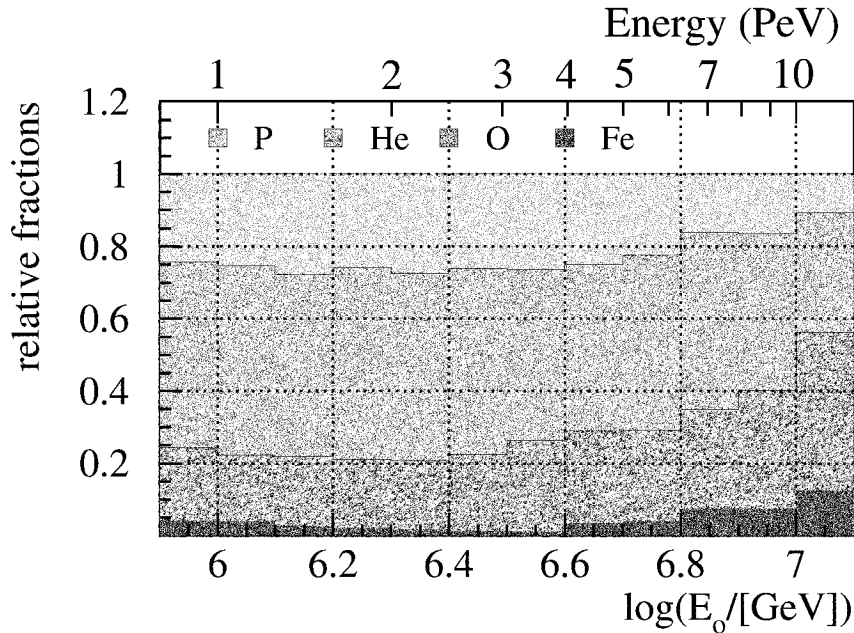


Fig. 7. The elemental composition of the cosmic ray spectrum in the region from $10^{15} - 10^{16}$ eV, measured by the KASCADE Collaboration [11]. The fractions of Helium, Oxygen and Iron have been normalized to the Hydrogen content. See text for details.

Additional evidence for this observation was provided by the KASCADE Collaboration [11]. Figure 7 shows the relative abundance of various elements as a function of energy, in the 1 – 10 PeV range. The fractions of all elements have been normalized to that of hydrogen. The figure shows an increase of the relative abundance of He, O and Fe beyond ~ 4 PeV. A *selective* reduction of the hydrogen content beyond the first kink would produce exactly this effect.

It is remarkable that the two kinks in the $\langle X_{\max} \rangle$ distribution coincide with the two “knees” observed in the all-particle energy spectrum itself (Figures 1 and 2). There is *no a priori* reason why that should be so. Note that there is *no* evidence for a kink in the $\langle X_{\max} \rangle$ distribution near the “ankle” at $10^{18.5}$ eV. This ankle, where the spectral index n changes from 3.3 back to its “canonical” value of 2.7 (see Figure

2), is usually interpreted as the point where cosmic rays of extragalactic origin start to dominate the galactic component. Below this energy, all charged particles are confined by the galactic magnetic field and, therefore, the particles that are the subject of our study are predominantly of galactic origin.

In Section 2.1, we ascribed differences in the precise energy at which the knee was found to different calibration procedures applied by the experimental groups active in this field. It should be emphasized that the two experiments that produced the data shown in Figure 6 are located at the same site and that the two Collaborations have overlapping membership. Therefore, it is unlikely that there are major systematic differences between the energy scales used in these two experiments. As a result, the *energy gap* between the two kinks in Figure 6 ($\Delta \log E = 1.8$) has most likely a much smaller systematic uncertainty than the energies at which the individual kinks are located. As discussed in the next section, this energy gap plays an important role in our explanation of all these experimental facts.

3 Relic neutrinos

3.1 Properties

According to the Big Bang model of the evolving Universe, large numbers of (electron) neutrinos and antineutrinos have been around since the beginning of time. In the very first second, when the temperature of the Universe exceeded 1 MeV, the density was so large that the (anti-)neutrinos were in thermal equilibrium with the other particles that made up the primordial soup: photons, electrons, positrons and nucleons. Photon-photon interactions created e^+e^- pairs, which annihilated into photon pairs. Interactions between (anti-)neutrinos and nucleons turned protons into neutrons and vice versa.

This *leptonic era* came to an end when the mean free path of the neutrinos become so large that their average lifetime started to exceed the age of the Universe, ~ 1 second after the Big Bang. Since that moment, the wavelengths of the (anti-)neutrinos have been expanding in proportion to the size of the Universe. Their present spectrum is believed to be a momentum-redshifted relativistic Fermi–Dirac distribution, and the number of particles per unit volume in the momentum bin $(p, p + dp)$ is given by

$$N(p)dp = \frac{p^2 dp}{\pi^2 \hbar^3 [\exp(pc/kT_\nu) + 1]} \left(\frac{g_\nu}{2}\right) \quad (3)$$

where g_ν denotes the number of neutrino helicity states [17]. The distribution is characterized by a temperature T_ν , which is somewhat lower than that for the relic photons. Since $(T_\nu/T_\gamma)^3 = 4/11$ and $T_\gamma = 2.726 \pm 0.005$ K [18], T_ν is expected to

be 1.95 K. The present density of these Big Bang relics is estimated at $\sim 100 \text{ cm}^{-3}$, for each neutrino flavor. That is nine orders of magnitude larger than the density of baryons in the Universe.

It is important to realize that, depending on their mass, these relic neutrinos might be very *nonrelativistic* at the current temperature ($kT_\nu \sim 10^{-4} \text{ eV}$). Since they decoupled, their momenta have been stretched by a factor 10^{10} , from $1 \text{ MeV}/c$ to $10^{-4} \text{ eV}/c$. If their rest mass were $1 \text{ eV}/c^2$, their maximum velocity would thus be $10^{-4}c$, or only 30 km/s.

The experimental upper limit on the mass of the electron antineutrino⁴ was recently determined at 2.2 eV (95% C.L.), from a study of the electron spectrum of ^3H decay [19]. The experimental results on atmospheric and solar neutrinos obtained by the Superkamiokande [20] and SNO [21] Collaborations suggest that neutrinos do have a nonzero rest mass. There is no experimental information that rules out a neutrino rest mass in the bracket $0.1 - 1 \text{ eV}$.

Despite their enormous abundance, estimated at $O(10^{86})$ for the Universe as a whole, relic neutrinos have until now escaped direct detection. The single most important reason for that is their extremely small kinetic energy, which makes it difficult to find a process through which they might reveal themselves.

3.2 How to detect relic neutrinos?

Let us imagine a target made of relic $\bar{\nu}_e$ s and let us bombard this target with protons. Let us suppose that we can tune this imagined proton beam to arbitrarily high energies, orders of magnitude beyond the highest energies that can be reached in our laboratories. Then, at some point, the proton energy will exceed the value at which the center-of-mass energy of the $p - \bar{\nu}_e$ system exceeds the combined mass energy of a neutron and a positron. Beyond that energy, the inverse β -decay reaction

$$p + \bar{\nu}_e \rightarrow n + e^+ \quad (4)$$

is energetically possible.

The threshold proton energy for this process depends on the mass of the $\bar{\nu}_e$ target particles. If this mass is large compared to the 10^{-4} eV kinetic energy typically carried by the target particles, this may be treated as a stationary-target problem, and the center-of-mass energy of the $p - \bar{\nu}_e$ system can be written as

$$E_{\text{cm}} = \sqrt{m_p^2 + m_\nu^2 + 2E_p m_\nu} \approx \sqrt{m_p^2 + 2E_p m_\nu} \quad (5)$$

⁴ In the following, we express masses in energy units, omitting the c^{-2} factor.

since $m_\nu \ll m_p$. When the experimental mass value of the proton (938.272 MeV) is substituted in Equation 5 and the requirement is made that $E_{\text{cm}} > m_n + m_e$ (940.077 MeV), this leads to

$$E_p m_\nu > 1.695 \cdot 10^{15} \text{ (eV)}^2 \quad (6)$$

This process will thus take place when

$$E_p(\text{eV}) > \frac{1.695 \cdot 10^{15}}{m_\nu(\text{eV})} \quad (7)$$

In our *Gedanken experiment*, this threshold would reveal itself through a decrease in the fraction of beam protons that traversed the target without noticing its presence, as E_p is increased beyond the threshold. We notice that the knee at 3 PeV exhibits exactly the features that we expect to see in this experiment: The particle flux suddenly starts to decrease when the threshold is passed. Therefore, we postulate the following hypothesis:

The change of the spectral index in the all-particle cosmic ray spectrum at an energy of ~ 3 PeV is caused by the onset of the reaction $p + \bar{\nu}_e \rightarrow n + e^+$, which becomes energetically possible at this point.

This hypothesis necessarily implies (Equation 7) that the mass of the electron neutrino equals ~ 0.5 eV. Also, the knee would have to be an *exclusive feature of the proton component* of the cosmic ray spectrum, if the hypothesis were correct. Beyond 3 PeV, one would thus expect to see a gradual drop in, for example, the p/α or p/Fe event ratios, as exhibited in Figure 7.

If protons interact with the relic background neutrinos, other cosmic ray particles may as well. The equivalent reactions in which α particles are dissociated in collisions with relic neutrinos and antineutrinos



have Q -values of 27.5 MeV and 30.1 MeV, respectively. The threshold energies for these reactions are larger than the threshold energy for reaction (4) by factors of 60.7 and 66.4, respectively.

If we now replace the imagined proton beam in our *Gedanken experiment* by a beam of α particles and the $\bar{\nu}_e$ target by one that consists of a mixture of ν_e and $\bar{\nu}_e$, we may expect to see the following when the beam energy is increased. As the energy exceeds the thresholds for the mentioned reactions, α particles will start to disappear from the beam. They are replaced by protons and neutrons. The neutrons

decay after a while into protons, so that each α particle turns into 4 protons, each of which carries, on average, 1/4 of the energy of the α particle. As the beam energy increases, an increasing fraction of the α s will undergo this process and the beam is thus increasingly enriched with protons.

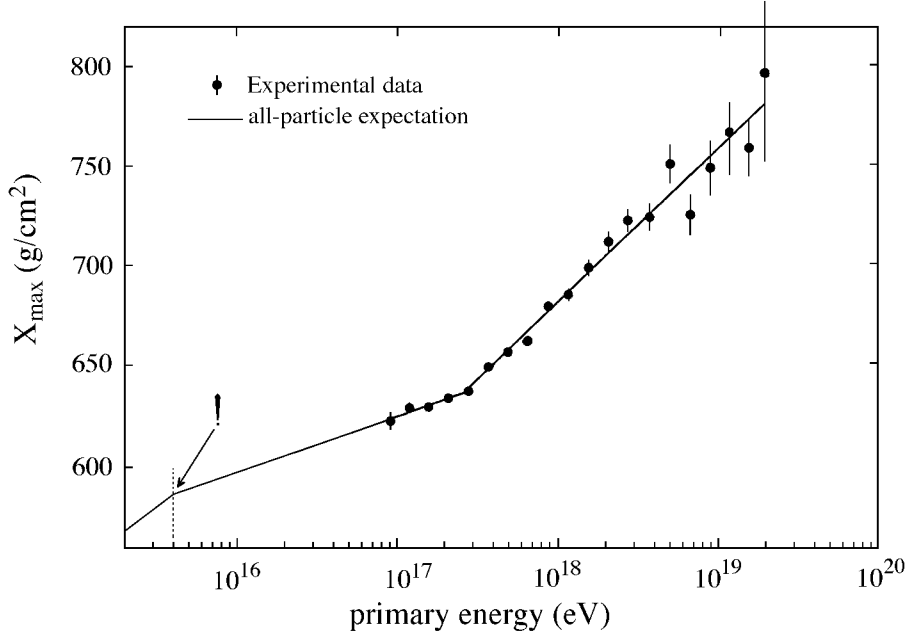


Fig. 8. The expected average depth of the shower maximum in the atmosphere (a) and the expected spectral index (b), as a function of the energy of the cosmic rays, predicted on the basis of extrapolations of experimental data obtained with the Fly’s Eye detector [22]. See text for details.

Also this scenario is in detailed agreement with the experimental cosmic ray data at energies above 10^{17} eV. At 100 PeV, the cosmic ray spectrum is dominated by α particles, since the protons have fallen victim to reaction (4). However, as the threshold near 300 PeV is crossed, α s start to disappear and are increasingly replaced by protons.

We would like to point out that this explanation of the cosmic ray data in the 0.1 – 1000 PeV energy range was already proposed at a conference in 1999 [22]. At that time, neither the CASA-BLANCA (Figure 6) nor the KASCADE (Figure 7) results were in the public domain. Based on the data available at that time, the kink in the $\langle X_{\max} \rangle$ distribution near 4 PeV was explicitly predicted, as illustrated in Figure 8.

The precision of the *neutrino mass* value that can be derived from these data is directly determined by the precision with which the energy of the knee is known. The value of $E_{\text{knee}} = 3 \pm 1$ PeV, which we adopted on the basis of the different reported values (see Section 2.1), translates on the basis of Equation 7 into the following value for the ν_e mass: $m_{\nu_e} = 0.5 \pm 0.2$ eV/ c^2 . This value falls nicely within the narrowing window that is still allowed by explicit measurements of this mass.

It also falls within the window (0.1 - 1 eV/c²) implicated by models that explain the Super-GZK events through a process in which extremely energetic neutrinos of extragalactic origin interact with the relic neutrinos in our galaxy and produce Z⁰s [23].

The *energy gap* between the thresholds for the $p\bar{\nu}_e$ and $\alpha\nu_e, \bar{\nu}_e$ reactions is *independent of the neutrino mass*. It is only determined by the Q -values of the various reactions: $\Delta \log E = 1.78, 1.82$, in excellent agreement with the measured energy gap between the two kinks in the $\langle X_{\max} \rangle$ distribution ($\Delta \log E = 1.8$, see Figure 6). This is perhaps the most remarkable and strongest point in favor of the described scenario.

4 A possible scenario for PeV cosmic ray production

We now turn our attention to an extremely crucial question: *How could the process that forms the basis of our hypothesis (inverse β -decay) play such a significant role, given its extremely small cross section?*

The cross section for $\bar{\nu}_e$ scattering off protons was measured for energies just above the threshold ($Q = 1.805$ MeV) to be [24]:

$$\sigma (\bar{\nu}_e + p \rightarrow n + e^+) \simeq 10^{-43} E^2 \text{ cm}^2 \quad (10)$$

where E is the $\bar{\nu}_e$ energy, expressed in units of MeV. If $m_{\nu_e} \approx 0.5$ eV, the cross section for the process $p + \bar{\nu}_e \rightarrow n + e^+$ is expected to scale with E_p^2 for protons in the energy range between 10^{16} eV and 10^{17} eV, where the effects of this process on the energy spectra and the elemental composition supposedly play an important role [25]. For a target density of $\sim 100 \nu_e \text{ cm}^{-3}$, the expected cross sections ($10^{-42} - 10^{-40} \text{ cm}^2$) translate into mean free paths of 10^{38-40} cm, or average lifetimes of 10^{20-22} years, *i.e.* 10 – 12 orders of magnitude longer than the age of the Universe. If this were all there is, the high-energy cosmic ion spectra could thus never have been affected at a significant level by the hypothesized processes.

However, it is important to realize that, with a mass of 0.5 eV, the relic $\bar{\nu}_e$ s would be *nonrelativistic* ($kT \sim 10^{-4}$ eV). Typical velocities would be < 100 km/s in that case [17], less than the escape velocity from the surface of the Sun. Such neutrinos may be expected to have accumulated in gravitational potential wells. Weiler [26] has estimated that the density of relic neutrinos in our own galaxy would increase by four orders of magnitude (compared to the universal density of 100 cm^{-3}) if their mass was 1 eV.

Locally, this effect could be much more spectacular. Extremely dense objects, such as neutron stars or black holes, could accumulate very large densities of relic neu-

trinos and antineutrinos in their gravitational fields. Let us consider, as an example, a typical neutron star, with a mass (M) of $3 \cdot 10^{30}$ kg and a radius of 10 km. Even at a distance (r) of one million kilometers from this object, the escape velocity is still considerably larger than the typical velocity of these relic neutrinos: 700 km/s.

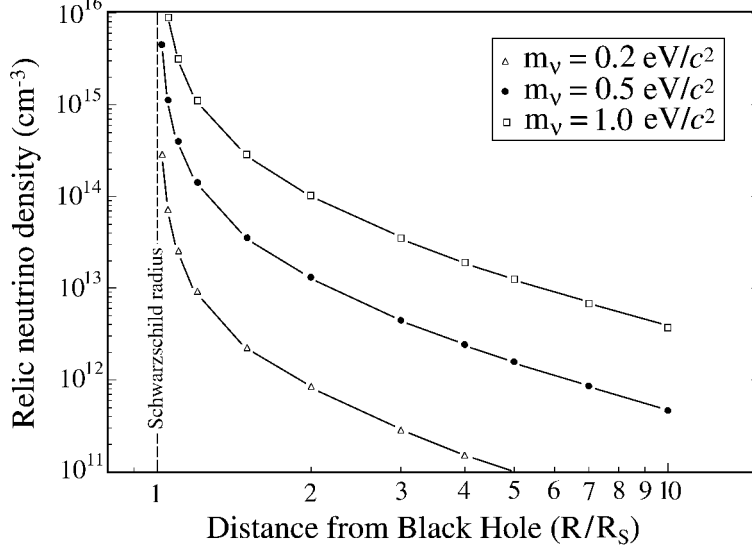


Fig. 9. The maximum density of neutrinos in the vicinity of a black hole, for different values of the neutrino mass. In calculating this density, all quantum states up to the Fermi level, determined by the local escape velocity, were assumed to be filled.

The concentration of relic neutrinos in such a local potential well is governed by the Pauli principle, which limits their phase-space density to $4g_\nu h^{-3}$ [17], where g_ν denotes the number of helicity states and h Planck's constant (see also Equation 3). Since the escape velocity scales with $r^{-1/2}$, the maximum neutrino density,

$$\rho_\nu(\text{max}) = \int_0^{p_{\text{esc}}} N(p) dp \sim p_{\text{esc}}^3$$

is proportional to $r^{-3/2}$, and reaches values of the order of 10^{12} cm⁻³ near the surface of this neutron star. If the source of the potential well has a different mass, the achievable neutrino density scales with $M^{3/2}$. In the “neutrino atmosphere” surrounding a massive black hole, the density may become as high as 10^{14} cm⁻³ near the Schwarzschild radius (see Figure 9). The average lifetime of a 10 PeV proton traveling in such an atmosphere would be of the order of 10^9 years, and correspondingly shorter for even higher energies (Equation 10).

This means that the accelerated cosmic protons would have to spend a very long time in this dense neutrino atmosphere in order to make the reaction $p + \bar{\nu}_e \rightarrow n + e^+$ a significant process. This would only be possible if the degenerate object in the center of this neutrino atmosphere were at the same time also the source of these accelerated particles. This might very well be the case [27]. Neutron stars

usually rotate very fast and exhibit very strong magnetic fields (up to $\sim 10^8$ T). When the magnetic axis does not correspond to the rotation axis, the changing magnetic fields in the space surrounding the neutron star may give rise to substantial electric fields, in which charged particles may be accelerated to very high energies. The synchrotron radiation emitted by accelerated electrons which constitutes the characteristic pulsar signature of these objects bears witness to this phenomenon. As an example, we mention the Crab pulsar, which is believed to be capable of accelerating protons to energies of 50 PeV and Fe ions to 1000 PeV [27].

So here follows our hypothesized scenario for the “Great Cosmic Accelerator”.

- During the gravitational collapse that led to the formation of a massive black hole somewhere in the center of our galaxy, large numbers of relic neutrinos were trapped in the gravitational field of this object. As in other processes that take place in the Universe, for example the Hubble expansion, all quantum states up to the Fermi level were filled and thus densities of the order of $10^{14-15} \text{ cm}^{-3}$ were reached near the Schwarzschild radius, R_S .
- Of course, also large numbers of protons and other ions present in the interstellar gas were gravitationally trapped in this event. However, these particles were subject to acceleration/deceleration in the very strong electromagnetic fields surrounding the newly formed black hole. In addition, they interacted with each other through the strong force. In the (long) time that has passed since the formation of the black hole, almost all these nuclei have either crashed into the black hole or escaped from its gravitational field.
- The only ions that did not undergo this fate are to be found in the equatorial plane, where they may be kept in closed orbits by the Lorentz force, since the magnetic field is perpendicular to this plane. This accretion disk of accelerated ions is the source of the PeV cosmic rays observed on Earth.
- The magnetically trapped ions could escape from their orbits in one of two ways:
 - A) Collisions with nuclei from the interstellar gas in the vicinity of the black hole. The cross section for this process is approximately energy independent.
 - B) Collisions with (anti-)neutrinos. The cross section for this process increases with the ion’s energy (Equation 10).
- The rates for these two processes are determined by the product of the cross section and the target density. Whereas the cross section of process A ($\sim 100 \text{ mb}$) is 16 orders of magnitude larger than that for process B (10^{-41} cm^2), the density of the relic neutrinos (10^{14} cm^{-3}) may well exceed the density of interstellar gas in the vicinity of the black hole by 16 *or more* orders of magnitude⁵. This would be the case if the latter density were $< 10^4$ atoms per cubic meter. In that case,

⁵ Note that the relic neutrinos are 9 orders of magnitude more abundant than protons in the Universe. This requirement is thus equivalent to an increase of the ν/p ratio by 7 orders of magnitude as a result of gravitational trapping.

the probabilities for the two processes are compatible and, therefore, they are in competition with each other.

- Above the knee (3 PeV), the source is selectively depleted of protons, because of process B. Since the cross section for this process (and thus its relative importance, compared with process A) increases with energy, and since the more energetic particles are found in a region with higher ν density (Figure 9), the spectral index n of the all-particle spectrum changes abruptly, from 2.7 to 3.0.
- Above the second knee, the source is *in addition* selectively depleted of α s, and the slope parameter increases further, from 3.0 to 3.3.

In this scenario, the magnetically trapped ions would have to orbit the black hole for a long period of time before escaping, typically $\sim 10^9$ years. One may wonder how that could be possible, since the effects of synchrotron radiation, which are certainly non-negligible for these high-energy protons, might destabilize the particle orbits. In order to calculate these effects, we need to know the radial dependence of the magnetic field strength, $B(r)$. In the following, we will assume that $B(r) = B_0 r^{-3}$, as for the dipole fields generated by rotating neutron stars. Charged particles with momentum p and charge Z are then kept in a circular orbit by the Lorentz force if

$$pr^2 = B_0 Z \quad (11)$$

Therefore, a loss of momentum, by synchrotron radiation, would increase the radius of the particle's orbit, but would otherwise not distort the stability of the system. At the same time, such an increase would change the magnetic flux through the current loop represented by the orbiting particle and the resulting emf would re-accelerate the particle such as to prevent the change in its orbit (Lenz's law).

The same feedback principle is applied in high-energy electron accelerators where synchrotron radiation losses are an important factor. For example, the LEP e^+e^- storage ring at CERN operated during its last year at energies in excess of 100 GeV. At that energy, the (average) synchrotron radiation loss amounted to 2.8 GeV per orbit. On average, this energy loss was compensated for by means of RF power. However, fluctuations about this average, which between two consecutive RF cavities were of the same order as the average energy loss itself, would rapidly lead to an increase in the transverse emittance of the beam, in the absence of a feedback mechanism. Yet, the LEP beam could easily be kept stable for a period of 24 hours. During this period, which corresponds to $\sim 10^9$ particle orbits, (fluctuations in) the accumulated synchrotron radiation losses amounted to $\sim 10^7$ times the particle's nominal energy.

Let us now consider, as an example, a black hole with a mass of $10^6 M_\odot$ ($R_S = 3 \cdot 10^9$ m). Let us assume that 10 PeV protons orbit this object at a distance of $10R_S$. A magnetic field with a strength of 1 mT would be needed to provide the centripetal force in that case. The protons would, on average, lose 2 GeV per orbit to

synchrotron radiation, an orbit which they complete in about 10 minutes. It would take such protons thus a period of $\sim 10^9$ years to accumulate a total synchrotron radiation loss equal to 10^7 times their own energy. Taking the LEP example as guidance, we conclude that such losses would not preclude orbit stability.

As the proton energy is further increased, the synchrotron radiation losses grow rapidly. In the above example, 100 PeV protons orbit the black hole at a distance of $\sqrt{10}R_S$, where the magnetic field strength is 32 mT. Since the specific energy loss dE/dx scales with $E^4 r^{-2}$, these protons lose energy to synchrotron radiation at a rate that is 10^5 times larger than that for the 10 PeV ones. Therefore, it takes them only 10^5 years to accumulate a total loss equivalent to 10^7 times their own energy. And although it might well be possible that their orbits are stable against the effects of synchrotron radiation for a much longer period of time, we cannot derive support for that from the LEP example, as we did for the 10 PeV protons. If the feedback mechanism were not capable to compensate completely for the synchrotron radiation losses, the particle would gradually spiral outward and end up in an orbit where it is (sufficiently) stable against any further energy losses.

Because of the mentioned dE/dx scaling characteristics of synchrotron radiation, it requires much less imagination to make the described scenario work for a supermassive black hole than for a black hole that resulted from the collapse of a massive star, say with a mass of $10M_\odot$ ($R_S = 3 \cdot 10^4$ m). In the latter case, the specific energy losses due to synchrotron radiation would be 10 orders of magnitude larger than in the previous examples. Thus, a 100 PeV proton orbiting such a black hole at a radius of $5R_S$ would lose energy at the prodigious rate of 40 TeV/m. It is unclear how and not very likely that in this case a stable configuration could be achieved that involves protons of such high energies.

One important aspect that we have not yet discussed is the power-law character of the energy spectra of the cosmic ray particles. Although the described scenario does not *guarantee* this characteristic feature of the experimental data, it can be shown that a reasonable choice of the boundary conditions does lead to a power-law spectrum with approximately the right spectral index. Equation 11 shows that if B behaves as a dipole field, the region between the radii $10R$ and R ($R > R_S$) could accommodate (ultrarelativistic) protons with energies between E_0 and $100E_0$, as well as heavier nuclei with energies between ZE_0 and $100ZE_0$. The most energetic particles would be found closest to the black hole. A constant density of accelerated particles throughout the accretion disk would then imply that $dN/dE \sim E^{-2.0}$. The effects of synchrotron radiation and aging of the black hole would lead to a further steepening of the spectrum, *i.e.* a further increase of the spectral index n . The first effect increases the particle density at lower energies (larger radii) at the expense of that at higher energies. The second effect is a consequence of the gradual increase in the total cross section observed in high-energy pp collisions [28]. As a result, the source spectrum is more depleted at higher energies (smaller radii), to an extent determined by the age of the black hole.

We would also like to point out that several pulsars are known to produce relativistic electrons with spectra that follow a power-law. These electrons are accelerated in the same em fields that form the basis of our scenario for PeV cosmic ray production.

Obviously, this scenario is not supported by observational evidence of the quality discussed in the previous sections. It is in fact little more than an imagined conspiracy of factors which, together, lead to measurable effects of a process that stopped playing a role in the Universe at large at the tender age of one second. However, it is *not inconceivable*, in the sense that no known physics principle is violated and no experimentally observed fact is ruled out. And apart from the fact that this scenario would make interactions between high-energy cosmic nuclei and relic neutrinos a significant process that would explain many features of the cosmic ray spectra in the energy range from 0.1 – 1000 PeV, it also has the merit that it provides an origin and an acceleration mechanism for the cosmic rays in this energy range. This in contrast with the Supernova shockwave acceleration models, which run out of steam in the 10^{14} eV region and do not offer any explanation for particles at higher energies.

5 Conclusions

The high-energy cosmic ray spectra exhibit some intriguing features that can all be explained in a coherent manner from interactions between cosmic protons or α particles and relic $\bar{\nu}_e$ s if the latter have a restmass of about $0.5 \text{ eV}/c^2$:

- Two “knees”, *i.e.* significant changes in the spectral index of the all-particle spectrum, which would correspond to the thresholds for the $p\bar{\nu}_e$ and $\alpha\bar{\nu}_e$ reactions.
- These knees coincide with kinks in the $\langle X_{\text{max}} \rangle$ distribution, which measures the average depth inside the Earth’s atmosphere at which the showers initiated by the cosmic rays reach their maximum intensity.
- The measured energy separation between these kinks ($\Delta \log E = 1.8$) is exactly what one would expect on the basis of the difference between the Q -values of the $p\bar{\nu}_e$ and the $\alpha\nu_e, \bar{\nu}_e$ reactions ($\Delta \log E = 1.80 \pm 0.02$).
- The kinks in the $\langle X_{\text{max}} \rangle$ distribution initiate changes in the elemental composition of the cosmic rays that are in detailed agreement with the changes one should expect when the thresholds for the $p\bar{\nu}_e$ and $\alpha\bar{\nu}_e$ reactions are crossed: A selective depletion of the proton component of the source spectrum at the first kink, a selective depletion of α particles combined with a reintroduction of protons at the second kink.

If collisions with relic neutrinos were indeed responsible for the described features, a large concentration of such neutrinos would have to be present in the vicinity of the source of the high-energy cosmic baryons, in order to explain the observed event

rates. We have shown that the required conditions could be met if charged particles accelerated and stored in the equatorial plane of a supermassive black hole in our galaxy were the source of the 0.1 – 1000 PeV cosmic rays measured here on Earth. This model could also explain the energy spectra of the hadronic cosmic rays.

If our model turned out to be correct, the PeV cosmic rays would provide the first direct measurement of a neutrino mass: $m_{\nu_e} = 0.5 \pm 0.2 \text{ eV}/c^2$. They would also provide evidence for a key aspect of the Big Bang model and thus offer a unique window on the leptonic era.

A crucial test of this model will be provided by the next generation of ^3H decay experiments. The proposed KATRIN experiment is designed to be able to measure a non-zero $\bar{\nu}_e$ mass down to values as small as $\approx 0.2 \text{ eV}/c^2$ [19] and should thus be in a position to either confirm or to rule out the mass value implied by our explanation of the experimental features of the PeV cosmic rays.

References

- [1] R. Blanford and D. Eichler, Phys. Rep. **154**, 1 (1987).
- [2] G.L. Cassiday, Ann. Rev. Nucl. Part. Phys. **35** (1985) 321.
- [3] J.W. Fowler *et al.*, *A Measurement of the Cosmic Ray Spectrum and Composition at the Knee*, preprint astro-ph/0003190, submitted to Astroparticle Phys., April 21, 2001.
- [4] R.M. Baltrusaitis *et al.*, Nucl. Instr. and Meth. **A240**, 410 (1985).
- [5] M. Nagano *et al.*, J. Phys. G **10**, 1295 (1984).
- [6] M. Amenomori *et al.*, Astrophys. J. **461**, 408 (1996).
- [7] S.P. Swordy and D.B. Kieda, preprint astro-ph/9909381 (1999).
- [8] D.J. Bird *et al.*, Astroph. J. **424**, 491 (1994).
- [9] A.A. Watson, Nucl. Phys. B (Proc. Suppl.) **22B**, 116 (1991).
- [10] K. Greisen, Phys. Rev. Lett. **16**, 748 (1966); G.T. Zatsepin and V.A. Kuz'min, JETP Lett. **4**, 78 (1966).
- [11] K. Bernlöhner *et al.*, Nucl. Phys. B (Proc. Suppl.) **85**, 311 (2000).
- [12] R. Wigmans, *Calorimetry, Energy Measurement in Particle Physics*, International Series of Monographs on Physics, Vol. 107, Oxford University Press (2000).
- [13] C. Caso *et al.*, Particle Data Group, Eur. Phys. J. **C15**, 1 (2000).
- [14] E. Longo and I. Sestilli, Nucl. Instr. and Meth. **128**, 283 (1975).

- [15] See <http://home.cern.ch/b/biebel/www/RPP00> for the numerical data used in this plot.
- [16] See <http://pdg.lbl.gov/xsect/contents.html>
- [17] S. Tremaine and J.E. Gunn, Phys. Rev. Lett. **42**, 407 (1979).
- [18] J.C. Mather *et al.*, Astrophys. J. **420**, 439 (1994).
- [19] A. Osipowicz *et al.*, *KATRIN: A next generation tritium β -decay experiment with sub-eV sensitivity for the ν_e mass*, e-print archive hep-ex/0109033.
- [20] Y. Fukuda *et al.*, Phys. Rev. Lett. **81**, 1562 (1998).
- [21] Q.R. Ahmad *et al.*, Phys. Rev. Lett. **87**, 071301 (2001); *ibid.* e-print archive nucl-ex/0204008.
- [22] R. Wigmans, *On Big Bang relics, the neutrino mass and the spectrum of cosmic rays*, Proceedings of the 6th Topical Workshop on Neutrino and Astroparticle Physics, San Miniato (Italy), 17-21 May 1999, Nucl. Phys. B (Proc. Suppl.) **85**, 305 (2000).
- [23] H. Päs and T.J. Weiler, Phys. Rev. **D63**, 113015 (2001); Z. Fofor, S.D. Katz and A. Ringwald, Phys. Rev. Lett. **88**, 171101 (2002).
- [24] D.H. Perkins, *Introduction to High Energy Physics*, 4th ed., Addison–Wesley (2000), p. 201.
- [25] P. Vogel and J.F. Beacom, Phys. Rev **D60**, 053003 (1999), and private communication.
- [26] T.J. Weiler, Astroparticle Physics **11**, 303 (1999).
- [27] A discussion about the possible role of neutron stars and black holes in the acceleration of high-energy cosmic rays can be found in: A.M. Hillas, Ann. Rev. Astron. Astrophys. **22**, 425 (1984).
- [28] R. Castaldi and G. Sanguinetti, Ann. Rev. Nucl. Part. Phys. **35** (1985) 351.